Green Chemistry

Uncovering the Active Sites and Demonstrating Stable Catalyst for the Cost-Effective Conversion of Ethanol to 1-Butanol

Journal:	*Green Chemistry*
Manuscript ID	GC-ART-06-2021-001979.R1
Article Type:	Paper
Date Submitted by the Author:	04-Aug-2021
Complete List of Authors:	Guo, Mond; Pacific Northwest National Laboratory, Chemical & Biological Processing Group; Washington State University, Chemical Engineering and Bioengineering Gray, Michel; Pacific Northwest National Laboratory, Chemical & Biological Processing Group Job, Heather; Pacific Northwest National Laboratory, Chemical & Biological Processing Group Alvarez-Vasco, Carlos; Pacific Northwest National Laboratory, Chemical & Biological Processing Group; Washington State University, Chemical Engineering and Bioengineering Subramaniam, Senthil; Pacific Northwest National Laboratory, Chemical & Biological Processing Group; Washington State University, Chemical Engineering and Bioengineering Zhang, Xiao; Washington State University, Chemical Engineering and Bioengineering; Pacific Northwest National Laboratory, Chemical & Process Development Group Kovarik, Libor; Pacific Northwest National Laboratory, Environmental Molecular Sciences Laboratory Murugesan, Vijayakumar; Pacific Northwest National Laboratory, Materials Sciences Phillips, Steven; Pacific Northwest National Laboratory, Chemical & Biological Processing Group Ramasamy, Karthikeyan; Pacific Northwest National Laboratory, Chemical & Biological Processing Group

ARTICLE

Uncovering the Active Sites and Demonstrating Stable Catalyst for the Cost-Effective Conversion of Ethanol to 1-Butanol

Received 00th January 20xx,
Accepted 00th January 20xx

DOI: 10.1039/x0xx00000x

Mond F. Guo,[1,2] Michel J. Gray,[1] Heather Job,[1] Carlos Alvarez-Vasco,[1,2] Senthil Subramaniam,[1,2] Xiao Zhang,[1,2] Libor Kovarik,[3] Vijayakumar Murugesan,[4] Steven Phillips,[1] and Karthikeyan K. Ramasamy[1,5]

The recent emergence of a robust renewable ethanol industry has provided a sustainable platform molecule toward the production of value-added chemicals and fuels; what is lacking now are viable conversion processes from ethanol that can displace the current production pathways from non-renewable pathways. Here in the work, we demonstrate the highly selective conversion of ethanol to higher alcohols over low copper loaded MgAl mixed oxide catalysts, with 50% improvement in higher alcohol yields over the current state of the art. At these copper concentrations, atomically dispersed Cu^{+1} were found to be stable even at highly reductive conditions and highly active towards higher alcohol products (e.g. butanol, hexanol) while suppressing side reaction pathways and leading to extended lifetimes of over 150 hours time on stream. Technoeconomic analysis conducted based on these experimental results demonstrate that this catalytic system is cost-competitive with the conventional process. This marks significant progress in the development of Guerbet coupling of ethanol as a viable renewable process and offers a pathway toward sustainable chemical and fuel production.

Introduction

The catalytic transformations of alcohols can provide a direct path towards the sustainable production of numerous commodity chemicals from renewable sources, replacing traditional petrochemical processes. The emergence of the bioethanol industry has made ethanol a more feasible candidate as a platform chemical, but effective catalytic processes remain lacking.[1-9] The coupling of ethanol is attractive for its facile C-C bonding which leads to valuable higher alcohols, yet its multi-step chemistry and susceptibility to side reactions (Scheme S1) has hindered progress towards higher yields and commercialization. Current strategies utilize multi-functional catalysts using tuneable supports with the acid/base surface chemistry necessary for aldol condensation, paired with a redox active catalyst to promote the initial dehydrogenation step.[10-13] This has enabled high product selectivities at mild conversions but maintaining those high selectivities at high conversions remains problematic. Controlling the reaction becomes challenging as the introduction of redox active materials not only can promote several new reactions, but their added presence on the catalyst surface necessarily alters the nature and balance of the tuned acid and base sites.

As an alternative approach, pursuing single atom catalysis provides an effective method to limit unnecessary active sites while maintaining sufficient catalytic efficiency. Rapid progress in this field towards the single-atom regime has already made clear the numerous advantages in activity, selectivity, stability, and precious metal economy.[14, 15] More importantly, this approach is also uniquely suited to addressing this particular chemistry, by restricting the number of catalytic sites that can participate in potential side reactions.[16, 17] Our approach was aimed at developing a catalyst that could selectively target the dehydrogenation of ethanol without significantly affecting the remainder of the reaction mechanism that leads to the higher alcohol formation.

In this study, we report an Mg/Al mixed oxide catalyst prepared with Cu^{+1} site in monoatomic form which minimizes copper (Cu) cluster formation during alcohol condensation reaction. We found that below a critical concentration, the dispersed Cu becomes stabilized on the support as an isolated monovalent site, resistant to further reduction and sintering even under highly reductive operating conditions, as shown by in-operando x-ray absorption spectroscopy (XAS) and high-angle annular dark-field scanning transmission electron microscopy (HAADF-STEM) study. The predominant Cu^{+1} species was found to be highly effective at improving conversion while maintaining higher alcohol selectivity, while

[1.] *Chemical & Biological Processing Group, Pacific Northwest National Laboratory, Richland, WA 99354, USA.*
[2.] *Voiland School of Chemical Engineering & Bioengineering Bioproducts, Science & Engineering Laboratory, Washington State University, 2710 Crimson Way, Richland, WA 99354, USA.*
[3.] *Environmental Molecular Sciences Laboratory, Pacific Northwest National Laboratory, Richland WA 99354, USA.*
[4.] *Materials Sciences, Pacific Northwest National Laboratory, Richland WA 99354, USA.*
[5.] *Correspondence and requests for materials should be addressed to K. K. (email: karthi@pnnl.gov).*

†Electronic Supplementary Information (ESI) available: [Data associate with ICP, XRD, XANES and EXAFS spectra]. See DOI: 10.1039/x0xx00000x

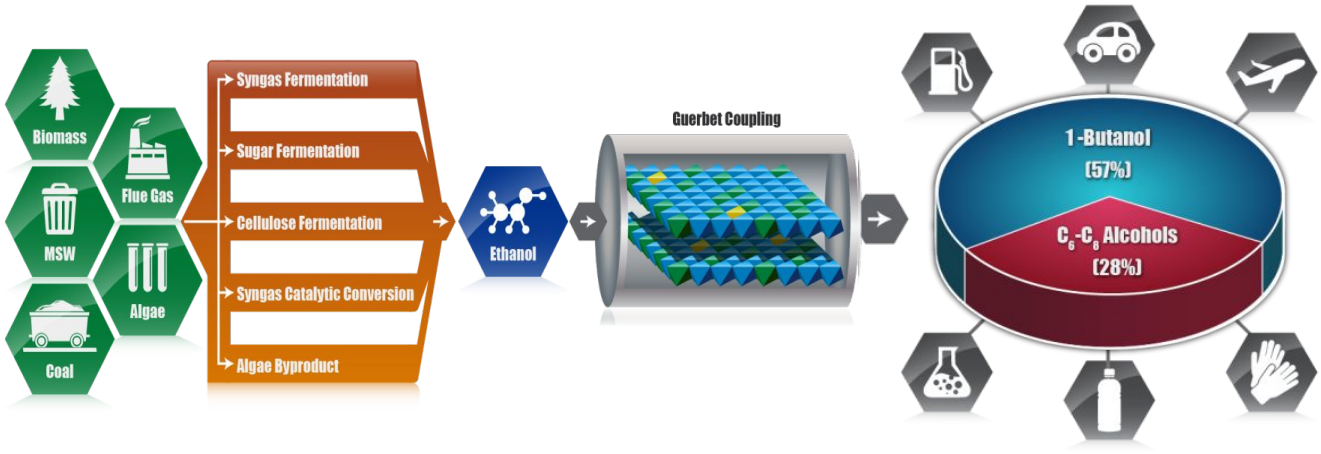

Fig. 1 Ethanol can be derived from a variety of traditional and renewable sources due to the development of flexible fermentation and conversion processes, positioning it as a promising intermediate platform molecule. Ethanol can be upgraded to a number of useful and valuable end products through the successful development of the Guerbet coupling process over low copper-doped Mg-Al layered double hydroxide-based catalysts. This process catalytically transforms ethanol in high selectivity (shown in Fig. 2b) and yield to higher alcohols such as 1-butanol, 1-hexanol and 2-ethyl-1-butanol which have numerous uses as plasticizers, polymer chemicals, and as potential fuel sources.

the appearance of Cu^0 at higher Cu concentrations coincided with a major shift towards reaction side products. Preventing the formation of Cu^0 allowed for unprecedented yields of higher alcohols from ethanol, (Figure 1, 2, and 4) with stable catalyst performance demonstrated over extended (>150 hours) lifetime runs. With nearly 50% total carbon yield to higher alcohols achieved in this work in a flow reactor system, this represents a significant improvement over reported state-of-the-art yields of ~40% in batch and ~30% in vapor phase continuous experiments (Table S1). This straightforward approach to achieving atomically dispersed and stable Cu^{+1} sites opens a novel pathway to overcoming many of the longstanding hurdles barring the development of viable catalytic processes toward alcohol condensation. Higher alcohols such as 1-butanol and 2-ethylhexanol have significant markets (3492 and 3771 metric tonnes per year, respectively) as plasticisers as well as intermediates in producing paints, adhesives, and coatings; [18-20] however, they are currently being generated by non-sustainable petrochemical processes or through ABE fermentation processes that require prohibitively energy intensive separations.[21, 22] The successful development of this catalytic system may lead toward the sustainable and cost effective production of a large sector of chemicals through renewable pathways.

Experimental Methods

Catalyst Synthesis

The CuMgAl layered double hydroxide (LDH) based catalyst was synthesized via the co-precipitation of metal salt precursors from a homogenous mixed and titrated solution.[23, 24] $Mg(NO_3)_2 \bullet 6H_2O$ and $Al(NO_3)_3 \bullet 6H_2O$ precursors were dissolved in aqueous solution in the desired stoichiometric Mg:Al ratio and pumped into a 333 K solution of $Na_2CO_3 \bullet 10H_2O$ that was titrated by 1 M NaOH, using a pH controller to automatically maintain a pH of 11. To introduce the Cu promoter, $Cu(NO_3)_2 \bullet xH_2O$ was added to the initial precursor solution to obtain a calculated Cu loading in weight percent of the final catalyst. Under steady titration and vigorous mixing, a precipitate suspension was formed that was then aged for 20 hours at 333 K. The precipitate was separated by filtration and washed with 333 K deionized water until ion concentrations dropped below 50 ppm in the wash effluent. The formed catalyst was dried overnight at 373 K, then pelletized at 16000 psig prior to calcination in air at 873 K for 2 hours with 4 K/min ramping, and subsequent sizing between 35-100 mesh sieves. Catalysts containing Cu were reduced in-situ by 50 mL/min of pure H_2 at ambient pressure for 80 minutes at 623 K prior to all experimental runs, and protected by N_2 or H_2 carrier gas at all times. All catalyst precursor materials were purchased from Sigma-Aldrich.

Characterization

Powder X-ray diffraction (XRD) was performed on a Phillips X-Pert diffractometer with Cu Kα radiation (λ ¼ 1.5437 Å) at 50 kV and 40 mA. XRD patterns were recorded at a 0.04° step size over a 5-100° 2θ range at 5 sec counting per step. Inductively coupled plasma (ICP) measurements were used to confirm the ratio of metals in the catalyst. Samples were prepared in a mixture of HNO_3 and HF (9.0 and 0.6 mL) before a second digestion in boric acid (5 mL) for complete dissolution at 383 K. The digested mixture was cooled to room temperature, diluted in water and analysed via ICP emission spectroscopy.

HAADF-STEM measurements were conducted with an FEI Titan 80-300 operated at 300 kV. The FEI Titan is equipped with CEOS GmbH double-hexapole aberration corrector for the probe forming lens, which allows imaging with ~0.1 nm resolution in STEM mode. The STEM images were acquired on a high angle annular dark field with an inner collection angle of 52 mrad. XAS measurements were performed at the Cu K-edge (8979 eV) in transmission mode. The samples were prepared by forming self-supporting wafers loaded into a 6 well sample

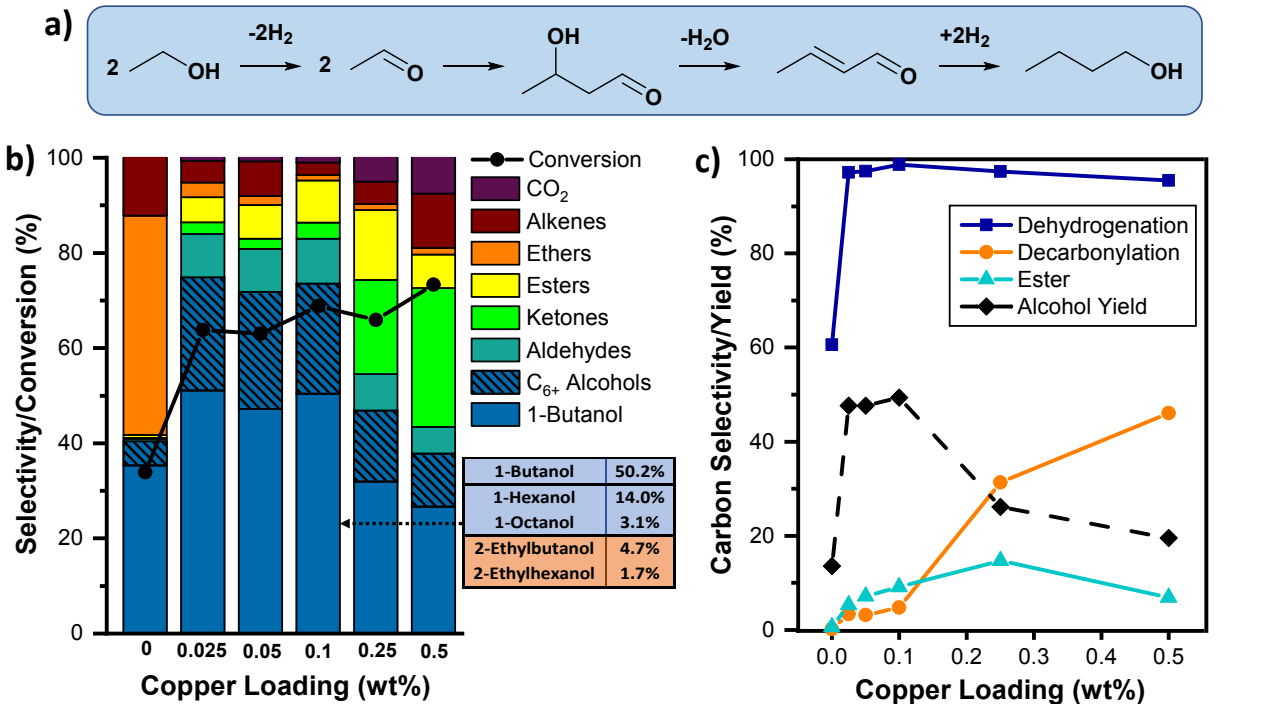

Fig. 2 a) Condensation pathway from ethanol to butanol b) Product distribution and conversion compared at varying Cu loadings at 598 K temperature, 300 psig H_2, 0.2 hr^{-1} weight hourly space velocity (WHSV) c) Alcohol product carbon yield and carbon selectivities towards major reaction pathways compared to copper loading

holder. The catalyst amount for each wafer was calculated to have an absorbance from 2-2.5 with an edge step of at least 0.2.

A scan range of -150 < E_0 < +800 eV was used to capture data in the EXAFS (extended X-ray absorption fine structure) range. The sample holder was loaded into a quartz tube reactor specifically prepared for in-situ measurements, sealed on both ends with Kapton windows using two Ultra-Torr fittings. Temperature was controlled by a large horizontal furnace around the reactor, and gas flow through the reactor was set by mass flow controllers. 100 sccm helium (He) was used for inert measurements. *In operando* measurements were performed under 20 sccm hydrogen (H_2) flow, which was bubbled through 200 proof ethanol to produce the reaction feed mixture. The Demeter XAS Data Processing software package, Athena and Artemis were used to process the data. XANES data was obtained from the normalized spectra -20 < E_0 < +50. EXAFS spectra were produced by removing the background using a fitted spline function, k^2-weighting, and Fourier transforming to R-space.

Catalytic Reaction

Experiments were performed in a fixed-bed tubular reactor using a down flow vapor-phase setup under 300 psig pressure maintained by a back pressure regulator. Catalyst was packed in the isothermal zone of 598 K maintained by a band heat, and ethanol was co-fed with of carrier gas (N_2 or H_2) across the bed. Product was separated into a gas and liquid phase via cold trap maintained at 277 K; gas product flow was measured by DryCal and analyzed by a gas chromatography-thermal conductivity detector (GC-TCD), while the condensed liquid products were identified via gas chromatography-mass spectroscopy (GC-MS) and quantitated by a flame-ionization detector (FID) using internal/external standards. Experiments were run for at least three days on stream, with regular gas sampling every 4 hours and liquid sampling every 24 hours to obtain a higher volume and improve mass and carbon balance. All reported data was taken at ~60 hours time-on-stream unless otherwise noted. Mass and carbon balances were calculated to be >95% and all selectivities are given on a carbon basis.

Results and Discussion

As shown in Figure 2a, Guerbet ethanol coupling goes through sequence of intermediate steps before generating the 1-butanol. The reaction intermediates makes it complicated to develop a catalyst that is selective to higher alcohols as the intermediate compounds acts as a branching point for the side product generation (Scheme S1), which are typically catalyzed by transition metal promoters.[24, 25] Homogenous catalytic methods have been shown to be successful in selective butanol synthesis,[26, 27] but do not have an easily scalable pathway towards industrialization. Heterogeneous catalysts design for the Guerbet reaction have thus focused mainly on two primary approaches.[10-13] One is forgoing transition metals and instead using the highly tunable hydroxyapatite material to catalyze all the steps required for the entire reaction pathway. This approach offers the highest reported selectivities to 1-butanol at the expense of conversion resulting from the limited dehydrogenation activity of hydroxyapatite.[28-31] While this is improved with promoted catalysts, the need to control the

resulting side product formation has led to research on a number of strategies to limit this additional impact of the promoter, such as focusing on metal-support interactions with CuCe-based catalysts,[13, 32] bimetallic formulations,[33-36] or physical mixtures that segregate the promoters from the active support.[37] However, no studies have focused on the minimization of the promoter as a method to address this challenge. Previous work has suggested that dehydrogenation activity is rapid and no longer rate limiting with copper promotion, and that highly dispersed Cu sites and the presence of Cu^{+1} can promote dehydrogenation activity. [38-40] Thus, minimizing the overall loading of copper metal to limit side product formation while simultaneously leveraging the improved activity of dispersed Cu sites appears to be a rational strategy to maintain alcohol selectivity at high conversions.

To test this, low concentration Cu promoted Mg/Al LDH catalysts were prepared. This support was chosen for its tunable nature[41] and long demonstrated activity toward the condensation reaction.[42-46] A set of catalysts were prepared via co-precipitation using a 4:1 molar ratio of Mg and Al to generate the LDH structure as noted in the catalyst synthesis section. Copper was added during the initial step to promote its replacement into the LDH structure as a solid solution, Different copper concentrations from 0.025wt% to 0.5wt% calculated by weight percent of the total metal content were prepared.

The performances of the catalysts for the aldol condensation of ethanol were evaluated in a pressurized packed bed flow reactor. The ethanol conversion and carbon selectivity of the products were analysed after 60 hours on stream to compare the reactions at steady state conditions, with the results are reported in Figure 2b and in greater detail in Table S2. Without Cu, the Mg-Al LDH based catalyst exhibits similar selectivity for both condensation products as well as for acid-catalysed dehydration products (Figure 2c), including the bimolecular dehydration to ether(s) or the unimolecular dehydration to alkene(s), which are generally dependent primarily on the reaction temperature and the strength of the acid site.[47, 48]

The addition of Cu significantly increases the alcohol condensation yield by raising ethanol conversion as well as the selectivity towards dehydrogenation products. In particular, results from the 0.1%Cu catalyst demonstrated for the first time high conversions levels (~65%) while simultaneously maintaining 75% carbon selectivity to higher alcohols. Even at 0.025% Cu loading, the catalyst was found to be sufficiently active toward dehydrogenation to nearly eliminate dehydration activity compared to the unpromoted catalyst. At the same time, Cu promotion led to the formation of ketone and ester side products that were otherwise essentially absent on the support Mg/Al LDH. However, adding Cu up to 0.1% loading had limited effect on generating these side products; as a result, the overall carbon yield to higher alcohols neared 50% for Cu loadings of 0.1% and lower. Increasing the Cu loading to 0.25% caused another significant shift in the product distribution, with selectivity towards ketones rising to 24.9% with a corresponding drop in the overall selectivity to alcohols to 49%, with this trend increasing 0.5%Cu loading. From Figure 2c, a very clear region of maximized alcohol yield is found at low copper concentrations, whereas the overall yield is increasingly compromised by ester and especially ketone product formation at higher Cu loadings.

Ester formation has been shown to be favourable over Lewis acid sites, which stabilizes the hemiacetal intermediate between an ethanol and acetaldehyde.[49-51] Previous work by has specified the active sites as the edge sites of Cu supported on zirconia.[52] Formation of ketone products occur on the Cu initially forming an aldol condensation intermediately followed by hydride shift and subsequent decarbonylation.[53-55]

Catalyst Characterization

XRD characterization of the un-calcined and calcined catalyst samples were used to verify the formation and incorporation of Cu into the solid solution (Figure S1). The actual metal content post-synthesis was measured by ICP shown in Table S3, which determined the final Mg/Al atomic ratio to be ~3.45, with Cu molar compositions between 0.04%-0.16% for the primary catalysts.

Investigation of the nature of the Cu sites was first attempted using typical analytical methods such temperature programmed reduction (TPR) and X-ray photoelectron spectroscopy (XPS). However, due to the low Cu concentration, TPR and XPS did not offer reliable results. In-situ XAS analysis was then utilized as the primary means of probing the location and characteristics of Cu in the catalyst. Comparing the XANES spectra of

Investigation of the nature of the Cu sites was first attempted using typical analytical methods such temperature programmed reduction (TPR) and X-ray photoelectron spectroscopy (XPS). However, due to the low Cu concentration, TPR and XPS did not offer reliable results. In-situ XAS analysis was then utilized as the primary means of probing the location and characteristics of Cu in the catalyst. Comparing the XANES spectra of the catalysts under H2 flow at 598 K, showing that there are no significant differences between them. (Figure 3a) The common features are the shoulder at 8986.6 eV, characteristic of Cu^{+2} species, and the pre-edge feature at 8977 eV indicating that the copper is located in a distorted structure.[56, 57] The similarities between the spectra confirms the distribution of the copper atoms in largely equivalent sites in the support structure for all copper concentrations. The higher edge energy compared to the Cu^{O} standard matches what is reported in literature for Cu substituted LDH.[58]

Exposure to in operando conditions revealed that the catalysts differed significantly according to their relative loading. The samples were ramped to 598 K from ambient under H2 flow at a rate of 20 K/min while taking fast XANES spectra and held there until stable before bubbling pure ethanol with the gas. The highest loaded 6%Cu catalyst was directly reduced to its final metallic Cu^{0} state during the ramping process, but the remaining catalysts all exhibited a step-wise transition process through the formation of Cu^{+1}, marked by the gradual disappearance of the 8977 eV pre-edge feature and the 8987 eV shoulder shown in Figure 4b, as well as a novel peak at 8982.7

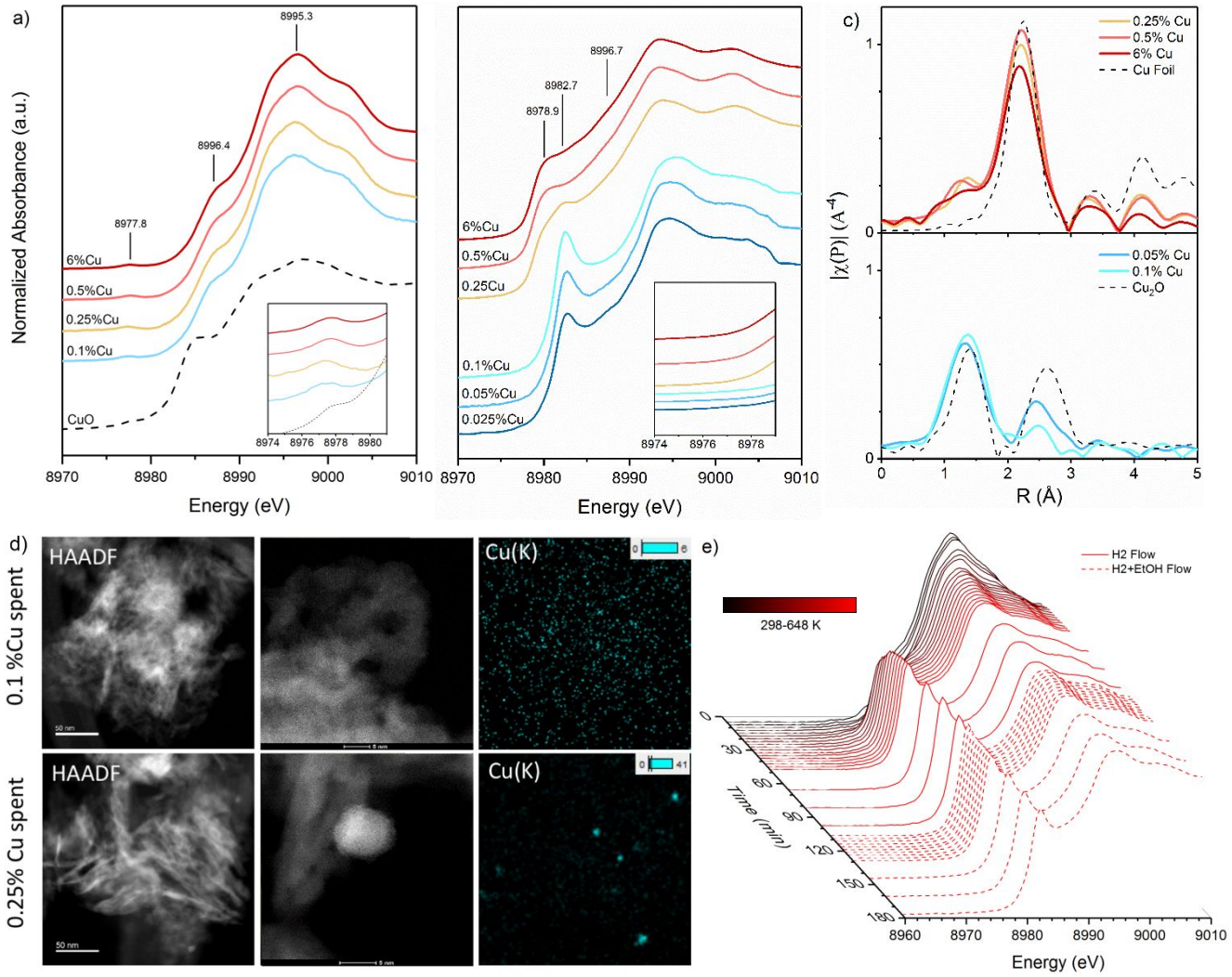

Fig. 3 a) Normalized Cu K-edge XANES spectra of Cu loaded catalysts under He flow at 598 K b) and *in operando* under H_2 and ethanol flow at 598 K c) Cu K-edge EXAFS (FT magnitude for Cu loaded catalysts *in operando* under H_2 and ethanol flow d) HAADF-STEM and corresponding Cu EDS mapping of spent 0.1%Cu and 0.25%Cu catalyst after >60 hours time on stream e) Normalized Cu K-edge XANES spectra of 0.1%Cu catalyst showing the stability of Cu^{+1} feature over time in *in operando* conditions

eV that is positioned slightly higher than the typical one at 8981 eV associated with Cu_2O.[59] At temperature, H2 flow was sufficient to fully reduce 0.5%Cu to Cu^0, but 0.25%Cu remained as a mix of Cu^{+1} and Cu^{+2} until the addition of ethanol.[60] Ease of reduction further decreased with Cu loading, marked by the diminishing magnitude of Cu^{+1} feature, with the remaining catalysts showing no signs of further reduction to Cu^0 despite extended exposure to H2 and ethanol flow. (Figure 3e) These result suggests that the catalytic activity of low Cu concentration catalysts could be primarily attributed to Cu^{+1} species and the relative absence of Cu^0.

The Fourier transformed EXAFS signal, plotted in R-space without phase-correction, shows the corresponding pattern with the diminishing magnitude of the Cu-O and Cu-Mg coordination shells concurrent with the change in Cu oxidation state and associated drop in the average Cu-O coordination number. (Figure 3c) The appearance of the Cu-Cu contribution peak at 2.54 Å indicated the clustering of copper in the higher loaded catalysts, and its absence for the 0.1%Cu catalyst confirming the stability of its Cu^{+1} sites below this copper concentration *in-operando*. HAADF-STEM was used to corroborate this by imaging catalysts obtained after extended reactions with run times greater than 100 hours; clear differentiation between spent 0.25%Cu and 0.1%Cu catalysts can be seen in Figure 3d. On the 0.25%Cu spent catalyst, numerous copper clusters were observed with particle sizes reaching up to 5 nm, while none were discovered on the 0.1%Cu catalyst with EDS mapping of copper indicating the same uniform dispersion as the fresh catalyst (Figure S2). The XAS data shows that while 0.25%Cu is noticeably mixed in both Cu speciation in the XANES as well as receiving contributions from both Cu-Cu and Cu-O shells in the FT-EXAFS data. Additionally, the lowest loading catalysts had retained the strongest Cu-Mg shell peaks in operando, indicating that a greater proportion of the copper remained as Cu^{+2} in the LDH lattice. Combined with the XAS results, this demonstrates that sufficiently low Cu

loadings below a certain threshold can be used to generate Cu sites that exist that predominantly atomically dispersed Cu^{+1} during reaction operation. This stark change in the copper oxidation state and physical nature provides an explanation for the significant shifts in the tested catalytic selectivities observed in the low copper loaded catalysts.

The stability of the Cu^{+1} site was demonstrated in operando for up to 11 hours in reductive conditions at the longest (Figure S4), and further tested by reoxidation cycling to verify the regeneration of the stable Cu^{+1} feature. 0.1% Cu samples retained after *in-operando* XAS measurements were reoxidized by exposure to air to avoid the replacement of copper into the lattice associated with oxidative thermal treatment. After 24 hours, the remeasured 0.1%Cu XANES spectra shows that the majority of the Cu^{+1} species were reoxidized to Cu^{+2}, with a minor Cu^{+1} population remaining as represented by a diminished 8982.7 eV peak and slightly lower edge energy. (Figure S5) Furthermore, the re-emergence of the same 8987 eV shoulder seen in the fresh catalyst signifies that the copper was reincorporated into LDH lattice in a similar fashion. In contrast, the XANES spectra of the reoxidized 0.25%Cu catalyst instead exhibits a new shoulder appearing at a lower energy, and its alignment with the same feature in CuO, reflecting irreversible Cu^0 clustering. (Figure S6-S7) The EXAFS data bears this out, showing the re-emergence of a significant second shell attributed to the Cu-Mg peak showing re-dispersion into the LDH matrix in the 0.1%Cu catalyst, compared to a completely absent second shell in the 0.25%Cu catalyst. (Figure S8)

To confirm this trend, another set of Cu on LDH catalysts were prepared using the wet impregnation method with copper concentrations between 0.05 wt% and 0.25 wt% to directly compare Cu speciation differences with the co-precipitated Cu LDH catalysts tested previously. In operando XAS of the impregnated samples shows that they are comparatively much easier to reduce, with the appearance of a strong Cu-Cu peak for impregnated catalysts with Cu loadings as low as 0.05% (Figure S9). Even in-situ conditions with flowing H2 was sufficient to produce an observable Cu-Cu bond in the EXAFS data for the 0.1%Cu impregnated catalyst. In operando XANES spectra for the impregnated catalyst much more closely resembles that of 0.25%Cu co-precipitated catalyst, with a mix of the Cu^0 and Cu^{+1} feature at 8979 ev and 8983 ev and the loss of the white line feature. The similarity in Cu speciation and morphological characteristics is reflected in the reaction results shown in Figure S10, where the increase in ester and ketone product selectivities when comparing co-precipitated and impregnated 0.1%Cu catalysts reflects the lack of atomically dispersed Cu character in the impregnated catalyst. At 0.25%Cu loading, Cu clustering occurs even on co-precipitated catalysts, and as a result the product profile is similar between the two preparation methods. The XAS results were confirmed by HADF-TEM imaging of the 0.1%Cu impregnated catalyst, where significant clustering was observed with particle sizes approximately 5 nm in diameter. (Figure S11-S13) From these comparisons, it can be seen that the initial dispersion of the catalyst and their relative spacing across the support plays a major role in preventing the formation of the copper clusters. In addition, even though both the XAS data and TEM images suggests that atomically dispersed species still exist in these less dispersed incipient wetness catalysts, the formation of aggregated copper has a dominant effect on the side product formation. Therefore, it can be seen that prevention of copper aggregation is critical to maintaining higher alcohol selectivity.

Catalyst Lifetime

Reaction studies were conducted to evaluate catalyst stability via lifetime experiments and to probe the nature of deactivation, particularly as Mg based catalysts are prone to deactivation. Extended catalyst testing across performed on different Cu wt% co-precipitated catalysts, with deactivation being primarily characterized by a steady drop in conversion along with a rise in dehydration product formation such DEE and small alkenes. The 0.1%Cu catalyst was shown to be extremely stable for over 150 hours time on stream, without significant changes to selectivity and overall yield. (Fig 4) At even higher time on streams, 0.1% Cu exhibited a slow monotonic decline in conversion over several hundred hours, with higher alcohols selectivity remaining above 74%.

Regarding the deactivation, metal particle growth is considered a major problem in supported catalysts, with Cu being particularly prone to rapid sintering at elevated temperatures.[61-64] Based on the previous XAS characterization of impregnated and co-precipitated Cu catalysts, aggregation of Cu over the course of the reaction is likely to both lower the overall catalytic activity as well as shift the product profile towards ketone and ester side products due to the change in Cu speciation. This effect was induced for a 0.1Cu co-precipitation catalyst by raising the initial pre-reduction temperature to 723 K where Cu sintering was certain to occur; as a result, selectivity to ketones and esters was roughly doubled with a corresponding decrease to alcohols, along with a loss in conversion when compared to the same reaction performed with the standard reduction protocol (Fig S15). Examining the deactivation profiles for the long-term tests shows that selectivities to both side-products trend downward over time alongside conversion, preserving the relative ratio to alcohol products. Furthermore, the lowest loaded Cu catalysts that were the most resistant to Cu clustering were the most susceptible to rapid deactivation. Combined with the lack of Cu aggregation observed in STEM-EDS of spent catalyst, this shows Cu sintering is unlikely to be a significant contributor to catalyst deactivation.

Deactivation can also occur through deposition of carbonaceous material through the production of excess unsaturated or highly reactive compounds, which polymerize to form the larger products that block the active sites.[38, 65] Thermogravimetric analysis of the deactivated catalyst, shown in Figure S16, revealed a total carbon deposition of 16.7 wt% on the catalyst. The carbonaceous material from the deactivated catalyst required a comparatively higher temperature, suggesting that higher molecular weight condensation products as the primary deactivating agent. This was further confirmed by the significant recovery of the catalyst activity and selectivity

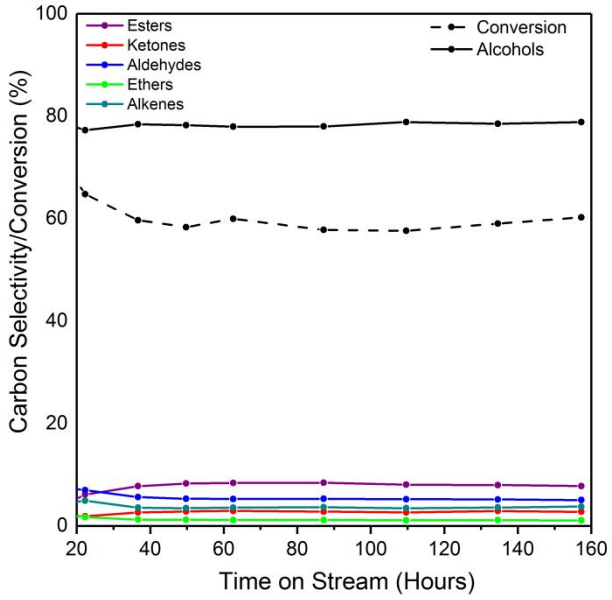

Fig. 4 Extended catalyst testing at 598 K temperature, 600 psig pressure H_2, 0.2 hr-1 weight hourly space velocity (WHSV) for 0.1% Cu loaded catalyst showing conversion and carbon selectivity of major product groups

could be obtained by calcining spent catalysts in air, an example of which is shown in Fig S17. The initial formation of these products is suppressed by rapid transfer hydrogenation step after the formation of crotonaldehyde. Hydrogenation of the aldehyde is catalysed over Lewis acid sites on the support via hydrogen exchange with a nearby alcohol through the Meerwein–Ponndorf–Verley (MPV) reaction.[10, 11] The internal C=C double bond hydrogenation was found to be carried out primarily through surface-mediated hydrogenation, as reported by Moteki et al.[31] Lower Cu loaded catalyst with predominantly Cu^{+1} sites were found to quickly deactivate with a corresponding increase in the unsaturated products; marked with the presence of unhydrogenated alkenes, followed by the appearance of butenol, butadiene, and benzenes towards the end of the deactivation. This suggests that while the Cu^{+1} sites may be sufficiently active for the initial dehydrogenation, they may be insufficient to catalyse the later hydrogenation steps and lead to rapid deactivation. Catalysts such as 0.25%Cu co-precipitated or 0.1%Cu impregnated that exhibited metallic Cu character were found to easily hydrogenate alkenes to alkanes and showed no deactivation changes over significant time, but at the cost of much greater selectivity to side products formation. (Fig S15) Thus, only a narrow Cu loading range around 0.1%Cu was found to be highly stable and highly selective to higher alcohols, suggesting that a finely tuned Cu concentration and speciation is required for optimal catalyst formulation.

Techno Economic Analysis

The key challenges to be overcome toward the commercialization of the Guerbet pathway are: 1) product selectivity and yield, 2) catalyst stability and lifetime, and 3) an effective separations process. Our work here has taken steps towards addressing the first two barriers, by demonstrating stable yields of >50% higher alcohols for extended time on stream. While development of this process remains at the bench-scale, recent progress made in this work has moved us forward to where consideration of the technical and economic hurdles leading to an industrial-scale process has become more necessary. A preliminary techno economic analysis was performed with the purpose of gauging the industrial viability of the current state of the process, as well as providing insight on the important technical and design variables and their impact on the process economics.

The base case is designed around 95% ethanol in water feed conversion to chemical-grade 1-butanol with a 1-hexene co-product (from 1-hexanol dehydration), using conversion and selectivity numbers measured during our long-term tests. In addition to 1-butanol the effluent also contains higher alcohols, water, H_2, and associated side products as measured in experiment, to be separated for either recovery, purification or purging as fuel gas. After identifying a number of potential azeotropes in this mixture, unit operations were specifically chosen to construct a realistic process to chemical-grade butanol based on the experimentally-derived product profile, without requiring technical development beyond the scope of the study. The azeotrope between the higher alcohols was addressed using a two-reactor system to convert part of the alcohols to alkenes and water. The alkenes and water formed 2 liquid phases that facilitated the removal of dehydration water. The alkenes were then catalytically reacted with the remaining higher alcohols to convert the branched alcohols into heavier ethers while leaving the 1-hexene co-product unchanged. The 1-hexene was purified by simple distillation. The detailed information on the configuration, relevant process data and catalyst cost development can be found in the Supplementary Information (Fig. S18, Table S4, Table S5)

Sensitivity analysis was performed around the following key factors that present potential major cost drivers: feed ethanol price, OPEX (operating expense), catalyst lifetime, 1-hexene market value, CAPEX (capital expense). The impacts on the minimum butanol selling price (MBSP) are shown in Figure 4. Total catalyst costs for the process was found to be a potential cost driver despite inexpensive Guerbet catalyst due to the inclusion of the additional catalytic steps required for co-product separations in the analysis. The MBSP is insensitive to the catalyst lifetime assuming it lasts at least 6 months. It can be seen that ethanol pricing has an outsized impact of the $0.55/lb MBSP when 1-hexene can be sold for $0.80/lb. The sale of 1-hexene co-product decreases the MBSP by about 10 cents per pound (20%). The calculated MBSP of $0.55/lb based on this work compares favourably with the 2017 1-butanol market price of ~$0.75/lb.

Overall, the ethanol price is the predominant factor in dictating the economic viability of the process, meaning higher alcohol selectivity remains the most critical area for improvement. The relatively low sensitivity of CAPEX and non-noble catalyst cost mean increasingly complex catalytic systems can be justified with catalytic improvements. This preliminary

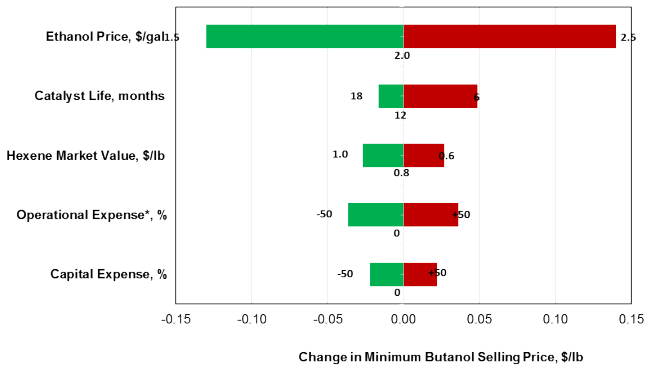

Fig. 5 Graphical representation of the Minimum Butanol Selling Price (MBSP) sensitivity to key economic factors varied around the base case values. *operational expense excluding ethanol cost and hexane credit.

study already shows that our currently achievable catalytic performance and stability can translate into an economically viable process. Though side product separation will likely always be necessary, continued development on understanding the mechanism as well as new catalytic approaches has made it easier to shape the product profile; catalyst design to avoid azeotrope issues or eliminate certain side reaction pathways altogether can improve the process economics further without pushing yield. In the same vein, the marginal cost of additional purification steps to obtain a co-product concurrent with butanol separation makes it appealing even with uncertainties in price. Considering the relative inhomogeneity of potential product profiles across the various catalytic approaches, consideration of the necessary auxiliary or downstream processes may support this technology to become more viable.

Conclusions

For the first time, conversion of ethanol to higher alcohols with simultaneously high yield and selectivity has been demonstrated. XAS work shows that stable Cu^{+1} species when presents at a sufficiently low loading is key factor in promoting high dehydrogenation rate while minimizing side product formation. In addition, catalyst stability was demonstrated without any change in performance for over 150 hours-time on stream. Beyond gaining new understanding of the Guerbet chemistry, this work also demonstrates the potential benefits from utilizing single-site catalysts to address problems related to selectivity. Based on this overall experimental data, a techno economic analysis was established. This analysis shows a currently market viable MSP of 0.55/lb for 1-butanol and identifies the need to consider downstream process units such as separations when advancing towards commercialization.

Author Contributions

M. Guo, M. Gray, H. Job, C. Alvarez-Vasco, and S. Subramaniam performed the experimental work. M. Guo, L. Kovarik, and V. Murugesan performed the catalyst characterization. S. Phillips performed the technoeconomic analysis. M. Guo, X. Zhang, V. Murugesan, S. Phillips, and K. K. Ramasamy contributed to the authorship of the manuscript.

Conflicts of interest

There are no conflicts to declare.

Acknowledgements

This work was financially supported by the U.S. Department of Energy (DOE), Office of Energy Efficiency and Renewable Energy, Bioenergy Technologies Office, and was performed at the Pacific Northwest National Laboratory (PNNL) under Contract No. DE-AC05-76RL01830 in collaboration with the Chemical Catalysis for Bioenergy Consortium (ChemCatBio), a member of the Energy Materials Network (EMN). This work was partly supported through the Co-Optimization of Fuels & Engines (Co-Optima) project sponsored by the U.S. Department of Energy, Office of Energy Efficiency and Renewable Energy, Bioenergy Technologies and Vehicle Technologies Offices. The views expressed in this article do not necessarily represent the views of the U.S. Department of Energy or the United States Government. The U.S. Government retains and the publisher, by accepting the article for publication, acknowledges that the U.S. Government retains a nonexclusive, paid-up, irrevocable, worldwide license to publish or reproduce the published form of this work, or allow others to do so, for U.S. Government purposes. This research was made possible by the valuable assistance of Dr. Tianpin Wu at the XSD Spectroscopy Group located in Sector 9 of the Advanced Photon Source (APS). This research used resources of the Advanced Photon Source, a U.S. Department of Energy (DOE) Office of Science User Facility operated for the DOE Office of Science by Argonne National Laboratory under Contract No. DE-AC02-06CH11357.

References

1. J. Sun and Y. Wang, *ACS Catalysis*, 2014, **4**, 1078-1090.
2. P. Alvira, E. Tomás-Pejó, M. Ballesteros and M. J. Negro, *Bioresource Technology*, 2010, **101**, 4851-4861.
3. B. Hahn-Hägerdal, M. Galbe, M. F. Gorwa-Grauslund, G. Lidén and G. Zacchi, *Trends in Biotechnology*, 2006, **24**, 549-556.
4. I.-C. Marcu, D. Tichit, F. Fajula and N. Tanchoux, *Catalysis Today*, 2009, **147**, 231-238.
5. E. C. D. Tan, L. J. Snowden-Swan, M. Talmadge, A. Dutta, S. Jones, K. K. Ramasamy, M. Gray, R. Dagle, A. Padmaperuma, M. Gerber, A. H. Sahir, L. Tao and Y. Zhang, *Biofuels, Bioproducts and Biorefining*, 2017, **11**, 41-66.
6. C. Smith, V. L. Dagle, M. Flake, K. K. Ramasamy, L. Kovarik, M. Bowden, T. Onfroy and R. A. Dagle, *Catal. Sci. Technol.*, 2016, **6**, 2325-2336.
7. R. A. Dagle, A. D. Winkelman, K. K. Ramasamy, V. Lebarbier Dagle and R. S. Weber, *Industrial & Engineering Chemistry Research*, 2020, **59**, 4843-4853.
8. S. Subramaniam, M. F. Guo, T. Bathena, M. Gray, X. Zhang, A. Martinez, L. Kovarik, K. A. Goulas and K. K. Ramasamy,

Angewandte Chemie International Edition, 2020, **59**, 14550-14557.
9. D. J. Gaspar, C. J. Mueller, R. L. McCormick, J. Martin, S. Som, G. M. Magnotti, J. Burton, D. Vardon, V. Dagle, T. L. Alleman, N. Huq, D. A. Ruddy, M. Arellano-Trevino, A. Landera, A. George, G. Fioroni, E. R. Sundstrom, E. Oksen, M. R. Thorson, R. T. Hallen, A. J. Schmidt, E. Polikarpov, E. Monroe, J. Carlson, R. W. Davis, A. Sutton, C. M. Moore, L. Cosimbescu, K. Kallupalayam Ramasamy, M. D. Kass, T. R. Hawkins, A. Singh, A. Bartling, P. T. Benavides, S. D. Phillips, H. Cai, Y. Jiang, L. Ou, M. Talmadge, N. Carlson, G. Zaimes, M. Wiatrowski, Y. Zhu and L. J. Snowden-Swan, *Top 13 Blendstocks Derived from Biomass for Mixing-Controlled Compression-Ignition (Diesel) Engines: Bioblendstocks with Potential for Decreased Emissions and Improved Operability*, Report PNNL-31421 United States 10.2172/1806564 PNNL English, ; Pacific Northwest National Lab. (PNNL), Richland, WA (United States), 2021.
10. J. T. Kozlowski and R. J. Davis, *ACS Catalysis*, 2013, **3**, 1588-1600.
11. D. Gabriels, W. Y. Hernandez, B. Sels, P. Van Der Voort and A. Verberckmoes, *Catalysis Science & Technology*, 2015, **5**, 3876-3902.
12. A. Galadima and O. Muraza, *Industrial & Engineering Chemistry Research*, 2015, **54**, 7181-7194.
13. W. Xianyuan, F. Geqian, T. Yuqin, J. Dahao, L. Zhe, L. Wenhua, L. Liu, T. Pengxiang, W. Hongjing, N. Jun and L. Xiaonian, *ChemSusChem*, 2018, **11**, 71-85.
14. J. Liu, *ACS Catalysis*, 2017, **7**, 34-59.
15. S. Zhang, L. Nguyen, J.-X. Liang, J. Shan, J. Liu, A. I. Frenkel, A. Patlolla, W. Huang, J. Li and F. Tao, *Nature Communications*, 2015, **6**, 7938.
16. M. Flytzani-Stephanopoulos and B. C. Gates, *Annual Review of Chemical and Biomolecular Engineering*, 2012, **3**, 545-574.
17. B. C. Gates, M. Flytzani-Stephanopoulos, D. A. Dixon and A. Katz, *Catalysis Science & Technology*, 2017, DOI: 10.1039/C7CY00881C.
18. J. Pafford, *Journal*, 2015.
19. L. Terry, *Journal*, 2015.
20. M. P. Malveda, S. Liu and Passarrat, *Journal*, 2015.
21. A. Oudshoorn, L. A. M. Van Der Wielen and A. J. J. Straathof, *Industrial & Engineering Chemistry Research*, 2009, **48**, 7325-7336.
22. A. Kujawska, J. Kujawski, M. Bryjak and W. Kujawski, *Renewable and Sustainable Energy Reviews*, 2015, **48**, 648-661.
23. S. Nishimura, A. Takagaki and K. Ebitani, *Green Chemistry*, 2013, **15**, 2026-2042.
24. I.-C. Marcu, N. Tanchoux, F. Fajula and D. Tichit, *Catalysis Letters*, 2013, **143**, 23-30.
25. C. Zhang, M. Borlik and H. Weiner, *Journal*, 2014.
26. S. Chakraborty, P. E. Piszel, C. E. Hayes, R. T. Baker and W. D. Jones, *Journal of the American Chemical Society*, 2015, **137**, 14264-14267.
27. H. Aitchison, R. L. Wingad and D. F. Wass, *ACS Catalysis*, 2016, **6**, 7125-7132.
28. C. R. Ho, S. Shylesh and A. T. Bell, *ACS Catalysis*, 2016, **6**, 939-948.
29. S. Ogo, A. Onda, Y. Iwasa, K. Hara, A. Fukuoka and K. Yanagisawa, *Journal of Catalysis*, 2012, **296**, 24-30.
30. A. G. Sato, D. P. Volanti, I. C. de Freitas, E. Longo and J. M. C. Bueno, *Catalysis Communications*, 2012, **26**, 122-126.
31. T. Moteki and D. W. Flaherty, *ACS Catalysis*, 2016, **6**, 4170-4183.
32. D. Jiang, X. Wu, J. Mao, J. Ni and X. Li, *Chemical Communications*, 2016, **52**, 13749-13752.
33. K. A. Goulas, S. Sreekumar, Y. Song, P. Kharidehal, G. Gunbas, P. J. Dietrich, G. R. Johnson, Y. C. Wang, A. M. Grippo, L. C. Grabow, A. A. Gokhale and F. D. Toste, *Journal of the American Chemical Society*, 2016, **138**, 6805-6812.
34. J. Shan, N. Janvelyan, H. Li, J. Liu, T. M. Egle, J. Ye, M. M. Biener, J. Biener, C. M. Friend and M. Flytzani-Stephanopoulos, *Applied Catalysis B: Environmental*, 2017, **205**, 541-550.
35. W. Y. Hernández, K. De Vlieger, P. Van Der Voort and A. Verberckmoes, *ChemSusChem*, 2016, **9**, 3196-3205.
36. Z. Sun, A. Couto Vasconcelos, G. Bottari, M. C. A. Stuart, G. Bonura, C. Cannilla, F. Frusteri and K. Barta, *ACS Sustainable Chemistry & Engineering*, 2016, DOI: 10.1021/acssuschemeng.6b02494.
37. S. Wang, K. Goulas and E. Iglesia, *Journal of Catalysis*, 2016, **340**, 302-320.
38. H. Yang, Y. Chen, X. Cui, G. Wang, Y. Cen, T. Deng, W. Yan, J. Gao, S. Zhu, U. Olsbye, J. Wang and W. Fan, *Angewandte Chemie*, 2018, **130**, 1854-1858.
39. M. E. Witzke, P. J. Dietrich, M. Y. S. Ibrahim, K. Al-Bardan, M. D. Triezenberg and D. W. Flaherty, *Chemical Communications*, 2017, **53**, 597-600.
40. I. C. Freitas, S. Damyanova, D. C. Oliveira, C. M. P. Marques and J. M. C. Bueno, *Journal of Molecular Catalysis A: Chemical*, 2014, **381**, 26-37.
41. D. P. Debecker, E. M. Gaigneaux and G. Busca, *Chemistry – A European Journal*, 2009, **15**, 3920-3935.
42. D. Stošić, F. Hosoglu, S. Bennici, A. Travert, M. Capron, F. Dumeignil, J. L. Couturier, J. L. Dubois and A. Auroux, *Catalysis Communications*, 2017, **89**, 14-18.
43. D. L. Carvalho, R. R. de Avillez, M. T. Rodrigues, L. E. P. Borges and L. G. Appel, *Applied Catalysis A: General*, 2012, **415-416**, 96-100.
44. J. I. Di Cosimo, Apesteguı, C. R.´a, M. J. L. Ginés and E. Iglesia, *Journal of Catalysis*, 2000, **190**, 261-275.
45. K. K. Ramasamy, M. Gray, H. Job, C. Smith and Y. Wang, *Catalysis Today*, 2016, **269**, 82-87.
46. W. Y. Hernández, J. Lauwaert, P. Van Der Voort and A. Verberckmoes, *Green Chemistry*, 2017, **19**, 5269-5302.
47. W. Knaeble and E. Iglesia, *The Journal of Physical Chemistry C*, 2016, **120**, 3371-3389.
48. P. A. Torresi, V. K. Diez, P. J. Luggren and J. I. Di Cosimo, *Catalysis Science & Technology*, 2014, **4**, 3203-3213.
49. G. Carotenuto, R. Tesser, M. Di Serio and E. Santacesaria, *Catalysis Today*, 2013, **203**, 202-210.
50. E. Santacesaria, G. Carotenuto, R. Tesser and M. Di Serio, *Chemical Engineering Journal*, 2012, **179**, 209-220.
51. K. Inui, T. Kurabayashi, S. Sato and N. Ichikawa, *Journal of Molecular Catalysis A: Chemical*, 2004, **216**, 147-156.
52. I. Ro, Y. Liu, M. R. Ball, D. H. K. Jackson, J. P. Chada, C. Sener, T. F. Kuech, R. J. Madon, G. W. Huber and J. A. Dumesic, *ACS Catalysis*, 2016, **6**, 7040-7050.
53. M. J. L. Gines and E. Iglesia, *Journal of Catalysis*, 1998, **176**, 155-172.
54. M. Neurock, Z. Tao, A. Chemburkar, D. Hibbitts and E.

Iglesia, *Faraday Discussions*, 2016, DOI: 10.1039/C6FD00226A.

55. M. E. Sad, M. Neurock and E. Iglesia, *Journal of the American Chemical Society*, 2011, **133**, 20384-20398.
56. C. Lamberti, S. Bordiga, F. Bonino, C. Prestipino, G. Berlier, L. Capello, F. D'Acapito, F. X. Llabres i Xamena and A. Zecchina, *Physical Chemistry Chemical Physics*, 2003, **5**, 4502-4509.
57. A. Dick, E. R. Krausz, K. S. Hadler, C. J. Noble, P. L. W. Tregenna-Piggott and M. J. Riley, *The Journal of Physical Chemistry C*, 2008, **112**, 14555-14562.
58. W. H. Cassinelli, L. Martins, M. Magnani, S. H. Pulcinelli, V. Briois and C. V. Santilli, *RSC Advances*, 2016, **6**, 20453-20457.
59. N. Hilbrandt and M. Martin, *The Journal of Physical Chemistry B*, 1999, **103**, 4797-4802.
60. W. Karim, C. Spreafico, A. Kleibert, J. Gobrecht, J. VandeVondele, Y. Ekinci and J. A. van Bokhoven, *Nature*, 2017, **541**, 68-71.
61. Z. Federica, S. Nicola and R. Nicoletta, *ChemCatChem*, 2018, **10**, 1526-1535.
62. T. W. Hansen, A. T. DeLaRiva, S. R. Challa and A. K. Datye, *Accounts of Chemical Research*, 2013, **46**, 1720-1730.
63. M. B. Gawande, A. Goswami, F.-X. Felpin, T. Asefa, X. Huang, R. Silva, X. Zou, R. Zboril and R. S. Varma, *Chemical Reviews*, 2016, **116**, 3722-3811.
64. R. van den Berg, T. E. Parmentier, C. F. Elkjær, C. J. Gommes, J. Sehested, S. Helveg, P. E. de Jongh and K. P. de Jong, *ACS Catalysis*, 2015, **5**, 4439-4448.
65. E. Simón, J. M. Rosas, A. Santos and A. Romero, *Catalysis Today*, 2012, **187**, 150-158.